Supra-subduction affinity in the Neoproterozoic serpentinites in the Eastern Desert, Egypt: Evidence from mineral composition

A.E.S. Khalil, M.K. Azer *

Geology Department, National Research Centre, Al-Behoos St., 12622 Dokki, Cairo, Egypt

Abstract

Serpentinites in the Eastern Desert (ED) of Egypt represent integral components of the ophiolites. Metamorphic textures of the serpentinites preserve the complex mineralogical evolution from primary peridotite through metamorphism, and late-stage hydrothermal alteration. Two textural types are distinguished in the olivines of the present serpentinized peridotites, namely (a) highly-strained olivine grains with kink bands, as in the deformed mantle tectonites from ophiolites, and (b) non-strained grains. The latter may represent recrystallized crystals during later thermal metamorphic events due to the intrusion of granite. On the basis of X-ray diffraction analysis, antigorite is the main serpentine minerals with lesser chrysotile and lizardite which indicates that serpentinites were formed under prograde metamorphism. Relict primary minerals of the serpentinites are Cr-spinel, olivine and pyroxene. Chrome spinel relicts have high Cr# (0.60–0.80), whereas primary olivines are Mg-rich nature (Fo = 89–96). Geochemical compositions of serpentinites indicate that they formed not at mid-ocean ridges but at spreading centers associated with subduction zones and this could have happened in a supra-subduction zone either in the fore-arc or back-arc environments. Mineral compositions of primary chrome spinels and olivines are similar to those of modern fore-arcs. High Cr# in the relict chrome spinels and Fo in the primary olivines of serpentinites indicate that they are residual after extensive partial melting and originated by sea-floor spreading during subduction initiation.
© 2007 Elsevier Ltd. All rights reserved.

Keywords: Serpentinite; Ophiolite; Chrome spinel; Olivine; Fore-arc

1. Introduction

The Arabian–Nubian Shield (ANS) is adorned with dismembered and altered ophiolites and ophiolite mélanges. This study concentrates on two ophiolite complexes at Um Khariga and Gebel Ghadir which are located in the central ED of Egypt. The ED ophiolites contain highly altered serpentinites and talc-carbonate rocks enclosing rare relics of fresh peridotite. Most recent studies of the Egyptian ophiolites infer formation in a supra-subduction zone setting (Abu El Ela, 1990; Khudeir and Asran, 1992; El-Sayed et al., 1999; Khalil, 2000; Ahmed et al., 2001, 2006; Abdel Aal et al., 2003; El Bahariya and Arai, 2003; Farahat et al., 2004; Azer and Khalil, 2005; El Gaby, 2005; Azer and Stern, 2007). Supra-subduction zone (SSZ) ophiolites have geochemical compositions which indicate that they were not formed at mid-ocean ridges but at spreading centers in fore-arc or back-arc convergent margin settings.

Serpentinites represent the most characteristic lithological unit in the Pan-African dismembered ophiolite sequence exposed in the ED of Egypt. Serpentinite exposures are usually aligned along major suture zones or thrust faults separating the pre-Pan-African infrastructure from the overlying Pan-African suprastructure. The geological studies carried out on the serpentinites in the ED concentrated mainly on their geology, petrography and bulk chemistry. However, information about the parent ultramafic protoliths is generally scarce because of the rarity of ultramafic relics within the serpentinite masses. Chromite, along with scattered relics of olivines and

* Corresponding author. Tel.: +20 2 37742962; fax: +20 2 33370931.
  E-mail address: mokhles72@yahoo.com (M.K. Azer).

pyroxenes, is the only mineral from the original ultramafic rock that routinely retains its original igneous composition in the serpentinites. So, chemical compositions of relict chromite, olivine and pyroxene minerals in highly serpentinized peridotites are important for understanding the magmatic evolution and tectonic setting of the ophiolites, since analyses of ophiolitic peridotites from Egypt are rare. The present paper presents new petrological and chemical mineral analyses from the Um Khariga and Gebel Ghadir serpentinized peridotites in the central ED of Egypt in order to discuss their Petrogenesis.

2. Field and previous work

The serpentinites at Um Khariga and Gebel Ghadir, the subject of the present work, lie in the central ED of Egypt (Fig. 1a). The previous studies carried out on the serpentinized peridotites from the two areas concentrated on their geology, petrography and bulk chemistry. Ahmed (2005) considered the Um Khariga serpentinites to have been derived from a non-ophiolitic intrusive hot ultramafic magma, as they have notable thermal effect of high grade on the adjoining submarine lava flow sheets. Analyses of primary silicate minerals as well as spinel relicts in these serpentinites are lacking, although a few analyses about accessory chrome spinels in Um Khariga serpentinites are available (El Bahariya and Arai, 2003).

2.1. Um Khariga serpentinite

The serpentinites of Um Khariga form dissected elongated masses (Fig. 1b) tectonically emplaced within thrust bounded assemblages that include gneissose diorite plutons, the Sukkari metavolcanic rocks and the Um Khariga metapyroclastic rocks (Akaad et al., 1994). The serpentinites are generally massive, but became sheared and foliated along the peripheries of the serpentinite lenses. The foliation of the intensively sheared serpentinites is parallel to the schistosity of the surrounding metavolcanic rocks. Along shear zones, the serpentinite bodies are replaced by talc-carbonate rocks. Fresh relics of partly serpentinized harzburgite showing gradational boundaries with the serpentinites are recorded. Chromitite bodies in the form of tabular or lenticular shapes are randomly distributed and parallel the regional structures of the enclosing serpentinites.

2.2. Gebel Ghadir serpentinite

The Ghadir ophiolite occurrence is an outstanding example of the northernmost ophiolites in the Nubian Shield. This ophiolitic succession was first described by E1 Sharkawy and E1 Bayoumi (1979); and later subjected to many studies (e.g. El Bayoumi, 1980, 1983; Takla et al., 1982; Farahat et al., 2004). Ries et al. (1983) considered the Ghadir ophiolite as a part of a large shallow

dipping nappe resting on a basement with continental affinities. The nature of the footwall is still controversial, since there is no direct evidence for the presence of a pre-Pan-African continental crust in the ED. The low Sr initial ratios of 0.702–0.704 for most igneous rocks in the ED (Stern and Hedge, 1985) support an ensimatic environment. There is, however, a strong indirect evidence for the close proximity of a craton, as indicated by Pb isotopes (Stacey and Stoeser, 1983; Sultan et al., 1992) and by the ca. 1500 Ma old detrital zircons (Kröner et al., 1988; Wust et al., 1987). El Gaby et al. (1988) concluded that the presence of old continental crust underneath the ophiolites and volcano-sedimentary association in the ED can be indirectly inferred from the presence of molasse sediments which usually characterize continental margin orogenic belts.
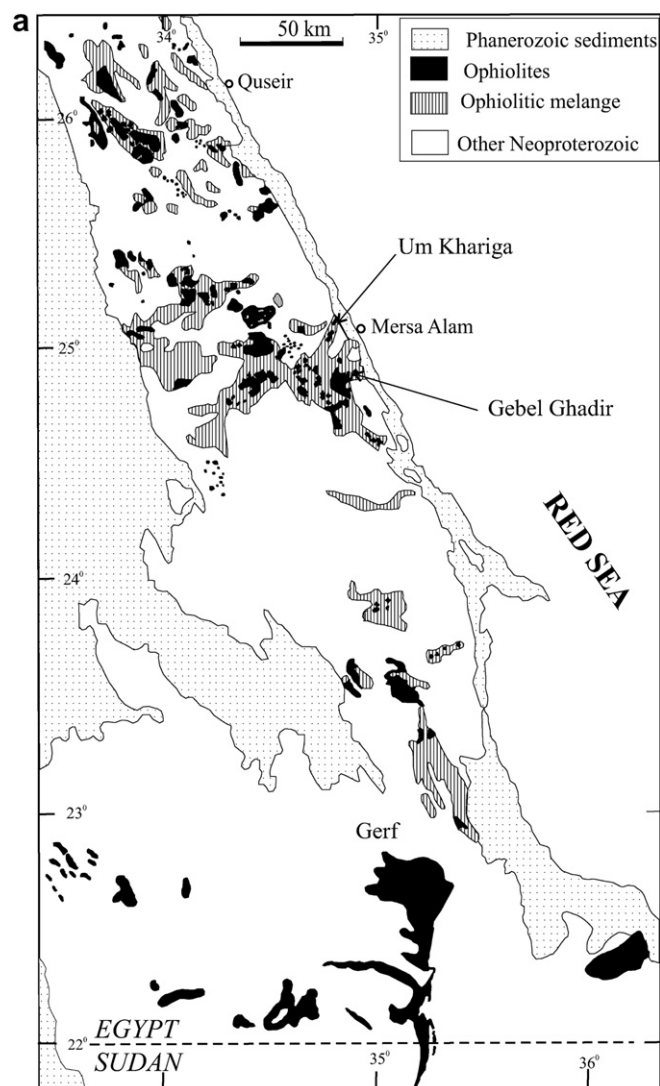

Fig. 1. (a) Distribution of ophiolitic rocks in the Eastern Desert of Egypt (modified after Shackleton, 1994). Localities of Um Khariga and Gebel Ghadir serpentinite bodies are shown on the map. (b) Geological map of Um Khariga area (after Akaad et al., 1994). (c) Geological map of Gebel Ghadir area (after Takla et al., 1982).
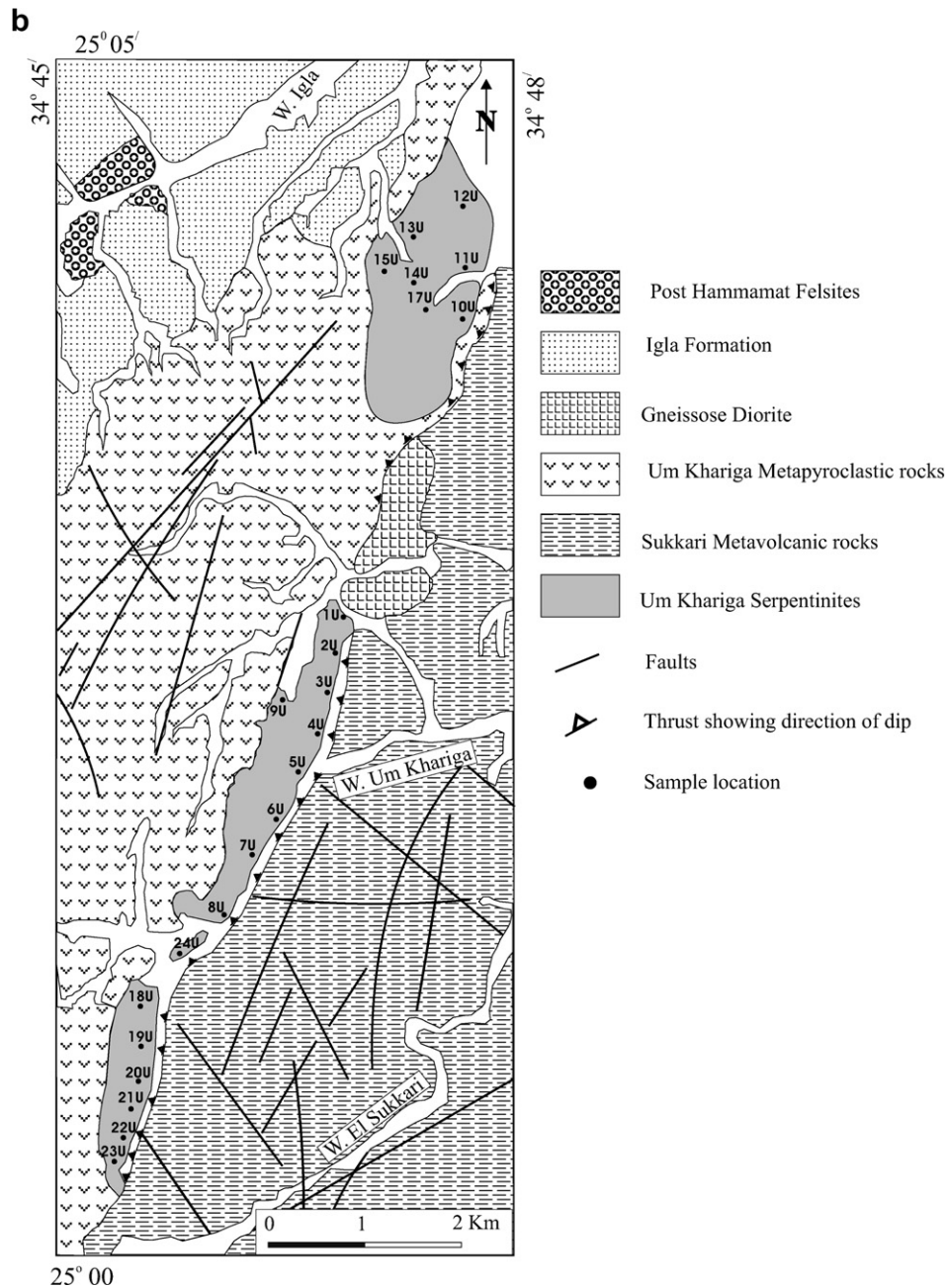
Fig. 1 (*continued*)

The ophiolitic rocks cropping out around Gebel Ghadir (Fig. 1c) include serpentinized peridotites and dunites, metagabbro, diabase and pillow lavas. They occur as fragments in a metasedimentary matrix that encompasses conglomerates, greywackes, mudstones, volcanoclastics and schists (Takla et al., 1982). The ophiolitic rocks are intruded by granites, as well as by a number of dykes. Gebel Ghadir serpentinites occur as large masses as well as small blocks incorporated into the ophiolitic mélange. The serpentinites represented by partly serpentinized peridotites and dunites, massive and sheared serpentinites and talc-carbonates. All the contacts of the serpentinite masses against the surrounding rocks are tectonic and marked by strong brecciation, shearing and cataclasis (Takla et al., 1982). Ophiolitic metagabbro occurs as small irregular masses associated with the serpentinites and as large bodies. Diabases occur as an elongated belt, trending NW-SE. Although, they appear in the field as large massive bodies, they are equivalent to the sheeted diabase dykes (Takla et al., 1982). Pillow lavas crop out in several occurrences. Chromitite lenses are encountered within the serpentinite masses. Also, thin pyroxenite dykes cut across the serpentinites. Magnesite occurs as veinlets and small pockets in the brecciated and sheared serpentinites.
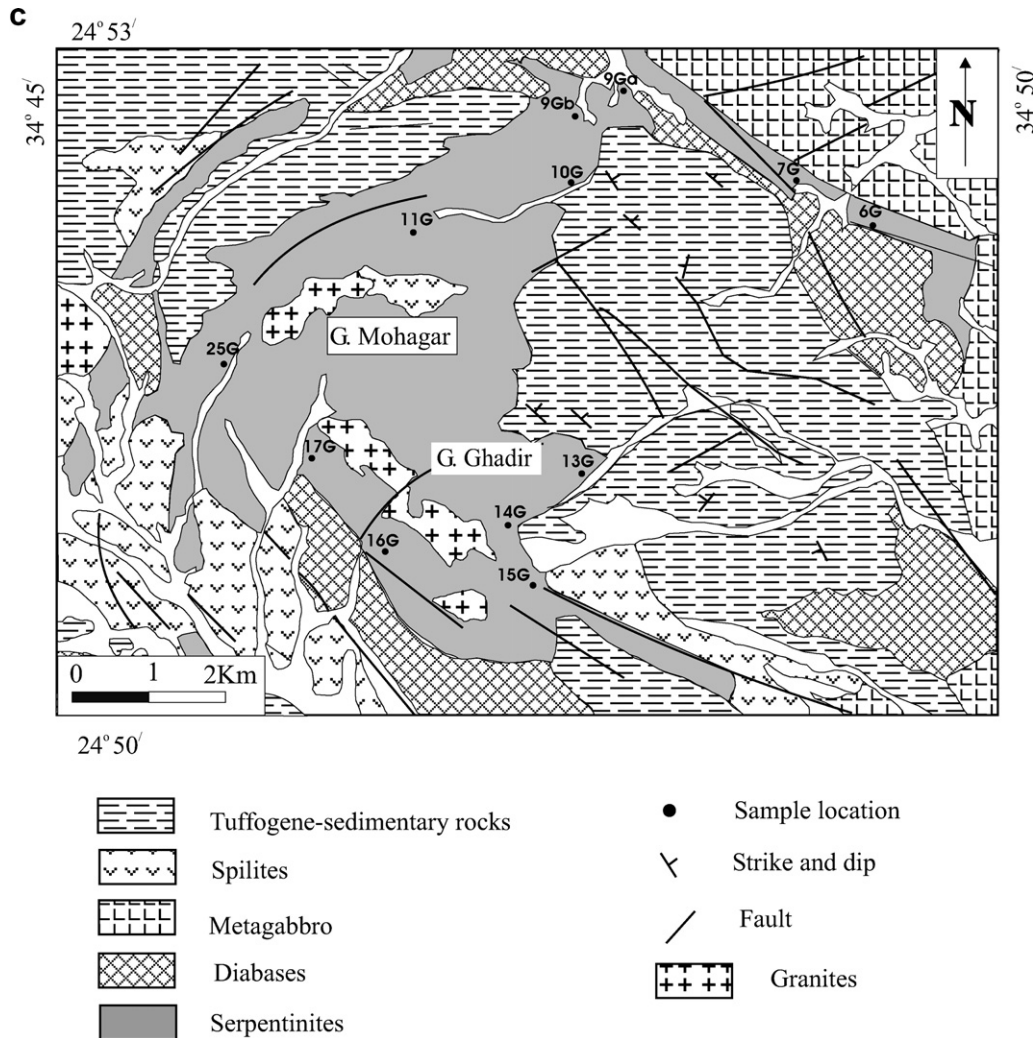
Fig. 1 (*continued*)

3. Analytical techniques

Chemical compositions of serpentines, chrome spinel, olivine and magnesite were determined using a CAMECA SV 50 electron microprobe under operating conditions of 15 Kv and 15 nA. Suitable synthetic and natural mineral standards were applied for calibration. The electron microprobe analyses were carried out on about 79 spots in different representative minerals in nine selected samples at Würzburg University, Germany. Major and trace elements were determined for 35 representative samples of massive serpentinites (23 Um Khariga and 12 Gebel Ghadir) by the X-ray fluorescence spectrometer (Philips Pw 2400) housed at the Institute of Geology and Mineralogy, Friederich-Alexander University, Erlangen-Nûrenberg, Germany. Concentrations of the major oxides were obtained on fused lithium-tetraborate discs, while the trace elements were determined on pressed pellets. Losses on ignition (LOI) were determined by heating powdered samples for 50 min at 1000 °C.

Some serpentinite samples were subjected to X-ray diffraction analysis to determine their mineralogical composition. The powder diffraction pattern of the samples was obtained with Cu radiation with secondary monochrometer. The scanning speed was $2\,\Theta = 1$ deg/min at constant voltage 40 Kv and 40 mA using BRUKUR D_8 advanced X-ray diffractometer. The identification of the minerals was carried out using the data given in the ASTM cards by measuring the d-values of the different atomic planes and their relative intensities.

4. Petrography

The Um Khariga and Gebel Ghadir serpentinites include massive and sheared varieties. Partly serpentinized peridotite and dunite, chromitite and talc-carbonates occur in subordinate amounts. The sheared serpentinites have the same mineralogical composition as the massive serpentinites, but the minerals in the former are commonly arranged in subparallel alignment producing the schistosity. Microscopically, there is a notable similarity in the mineralogy of the serpentinites in both localities. XRD data indicated that antigorite is the main mineral together with lesser chrysotile, lizardite and minor magnesite and

brucite. Chrysotile occurs as cross-fiber veinlets traversing the antigorite matrix, which indicates its late crystallization under static conditions.

Massive serpentinites commonly preserved crystal habits of orthopyroxene and olivine as well as the original rock texture, indicating harzburgite and dunite composition of the parent rocks; harzburgite dominates over dunite. The original orthopyroxene is indicated by the presence of bastite texture with very thin magnetite streaks and striations disposed along the cleavage planes of original orthopyroxene. Serpentinized olivine is indicated by presence of mesh texture that may be enclosing relicts of olivine crystals coated with iron oxides. Magnesite occurs as sparse crystals and fine aggregates in the massive serpentinites or as veinlets and pockets in the sheared varieties. The magnesite veinlets are monomineralic and cryptocrystalline with sharp contacts with the enclosing serpentinites. Brucite appears as platy or fibrous crystals intermixed with serpentines as well as veinlets. Chromite in the massive serpentinites occur as rounded, subrounded and irregular grains, while in the sheared varieties is mostly brecciated and rarely elliptical in shape. In some samples, chromite replaced by ferritchromite and magnetite. Magnetite was precipitated during the alteration of olivine and orthopyroxene and it commonly forms fine opaque clusters of tiny opaque crystals surrounding the altered primary mineral phases as well as veins.

Partly serpentinized harzburgite and dunite from Um Khariga and Gebel Ghadir consist essentially of serpentine minerals together with variable amounts of olivine, pyroxene, talc, magnetite and chromite. Olivine occurs in two textural types: (a) highly-strained olivine grains with kink bands, as in the deformed mantle tectonites from ophiolites, and (b) non-strained grains. The latter was observed only in the Gebel Ghadir serpentinites and may represent recrystallized crystals during later thermal metamorphic events due to the intrusion of granite. Chromitite lenses are composed of aggregates of coarse-grained chrome spinel crystals which are slightly altered along grain margins and cracks. Serpentine and minor magnetite and chlorite are common admixtures in the chromitite lenses. The chromitite lenses show common textures and structures such as cumulate and banding, typical of magmatic crystallization (Pal and Mitra, 2004). Foliated, fine-grained talc-carbonate rocks consist mainly of magnesite and talc together with minor serpentine and chromite. Pyroxenite dykes are scarce in the ophiolites and are composed almost entirely of orthopyroxene with variable amounts of actinolite, tremolite, chlorite and magnetite. They appear to represent later magmatic segregations intruded as dykes into the harzburgite and dunite tectonites (Khudeir, 1995).

5. Mineral chemistry

The whole-rock chemistry of the highly serpentinized peridotite is of limited geochemical use but the chemistry of preserved minerals, particularly olivine, spinel and pyroxene, reflects the magmatic conditions and the tectonic environment of the ultramafic parent rocks. Chemical com-

Table 1
Representative microprobe analyses of serpentine minerals from Um Khariga

Sample no.	5U					11U					3U		
Spot no.	p1	p2	p3	p4	p5	p1	P2	p3	p4	p5	p1	p2	p3
SiO_2	42.14	42.04	42.95	44.34	43.07	42.85	42.42	42.71	42.50	42.30	42.47	42.79	43.50
TiO_2	0.00	0.01	0.02	0.01	0.00	0.00	0.02	0.00	0.01	0.05	0.01	0.00	0.00
Al_2O_3	0.17	0.14	0.19	0.05	0.13	0.08	0.13	0.15	0.14	1.37	0.21	0.02	0.16
Cr_2O_3	0.05	0.09	0.00	0.01	0.08	0.06	0.09	0.12	0.04	0.70	0.03	0.03	0.06
MgO	41.19	42.05	41.82	39.50	40.84	41.80	40.50	40.95	40.39	41.16	42.11	41.74	40.83
CaO	0.04	0.05	0.01	0.00	0.00	0.03	0.00	0.04	0.00	0.00	0.01	0.09	0.05
MnO	0.00	0.00	0.04	0.00	0.03	0.00	0.01	0.02	0.05	0.04	0.07	0.11	0.08
FeO	2.55	2.26	2.27	2.52	2.45	1.72	2.36	1.47	2.11	1.41	1.36	1.97	1.44
NiO	0.33	0.38	0.18	0.32	0.24	0.28	0.26	0.35	0.23	0.17	0.15	0.12	0.12
Na_2O	0.01	0.00	0.00	0.00	0.03	0.00	0.00	0.06	0.00	0.00	0.00	0.00	0.07
K_2O	0.01	0.01	0.01	0.00	0.00	0.00	0.02	0.01	0.01	0.00	0.00	0.01	0.01
H_2O	12.72	12.84	13.12	12.68	12.89	12.43	12.59	13.19	12.98	12.95	13.19	12.54	12.82
Total	99.213	99.857	100.604	99.428	99.758	99.255	98.387	99.076	98.450	100.136	99.623	99.420	99.137
Structural formula based on 28 oxygens													
Si	7.946	8.041	8.215	8.198	8.203	8.073	8.083	8.129	8.225	8.023	8.269	7.997	8.137
Ti	0.000	0.001	0.003	0.001	0.000	0.000	0.003	0.000	0.001	0.008	0.002	0.000	0.000
Al	0.038	0.031	0.041	0.011	0.029	0.019	0.030	0.031	0.031	0.298	0.045	0.005	0.035
Cr	0.007	0.014	0.000	0.001	0.012	0.009	0.014	0.018	0.005	0.102	0.004	0.004	0.008
Mg	11.575	11.430	11.121	11.135	11.105	11.533	11.503	11.370	11.125	11.089	11.142	11.621	11.383
Ca	0.009	0.009	0.002	0.000	0.000	0.006	0.000	0.008	0.000	0.000	0.001	0.018	0.009
Mn	0.000	0.000	0.006	0.000	0.005	0.000	0.001	0.003	0.008	0.006	0.011	0.017	0.012
Fe	0.402	0.353	0.347	0.399	0.381	0.229	0.217	0.223	0.326	0.218	0.208	0.316	0.225
Ni	0.050	0.057	0.026	0.049	0.035	0.043	0.039	0.051	0.033	0.025	0.023	0.019	0.018
Na	0.004	0.000	0.000	0.000	0.011	0.000	0.000	0.022	0.000	0.000	0.000	0.001	0.025
K	0.003	0.001	0.001	0.000	0.000	0.000	0.004	0.002	0.001	0.000	0.001	0.002	0.003

Table 2
Representative microprobe analyses of serpentine minerals from Gebel Ghadir

Sample no.	6G					17G						13G				
Spot no.	p1	p2	p3	p4	p5	p1	p2	p3	p4	p5	p6	p1	p2	p3	p4	p5
SiO_2	43.63	42.82	44.00	43.71	42.73	43.42	43.05	42.15	43.76	43.26	43.14	42.09	42.65	43.89	43.50	43.19
TiO_2	0.01	0.00	0.01	0.00	0.02	0.00	0.01	0.00	0.03	0.00	0.01	0.00	0.00	0.03	0.01	0.01
Al_2O_3	0.12	0.17	0.17	0.09	0.45	0.09	0.17	0.09	0.57	0.12	0.12	0.16	0.09	0.79	0.13	0.22
Cr_2O_3	0.03	0.05	0.05	0.05	0.24	0.05	0.05	0.04	0.25	0.09	0.00	0.07	0.04	0.36	0.05	0.10
MgO	40.93	41.01	40.93	39.76	42.00	40.54	41.02	41.79	40.55	41.40	40.66	41.62	41.29	40.13	40.68	40.99
CaO	0.05	0.04	0.03	0.00	0.01	0.01	0.03	0.07	0.00	0.02	0.01	0.05	0.07	0.00	0.03	0.02
MnO	0.09	0.04	0.02	0.02	0.03	0.01	0.01	0.09	0.05	0.01	0.02	0.00	0.09	0.06	0.04	0.04
FeO	1.67	1.99	2.27	2.49	1.59	2.13	2.36	1.71	1.63	1.68	2.40	2.40	1.71	1.39	1.98	1.91
NiO	0.14	0.22	0.28	0.28	0.25	0.28	0.30	0.12	0.18	0.28	0.25	0.35	0.12	0.16	0.24	0.24
Na_2O	0.00	0.04	0.00	0.02	0.02	0.01	0.00	0.04	0.00	0.02	0.00	0.01	0.04	0.00	0.01	0.01
K_2O	0.01	0.01	0.01	0.00	0.01	0.00	0.01	0.01	0.00	0.01	0.00	0.01	0.01	0.00	0.01	0.01
H_2O	12.86	12.77	12.98	12.78	12.93	12.67	12.89	12.68	13.04	12.77	12.90	12.78	13.18	13.07	12.84	12.87
Total	99.52	99.17	100.73	99.19	100.26	99.21	99.89	98.78	100.07	99.67	99.52	99.54	99.28	99.88	99.50	99.61
Structural formula based on 28 oxygens																
Si	8.133	8.042	8.128	8.201	8.115	8.158	8.067	8.067	8.172	8.122	8.207	7.994	8.067	8.146	8.126	8.118
Ti	0.001	0.000	0.002	0.001	0.003	0.000	0.001	0.000	0.004	0.001	0.002	0.001	0.000	0.005	0.001	0.001
Al	0.025	0.037	0.036	0.020	0.098	0.020	0.037	0.020	0.125	0.027	0.026	0.035	0.020	0.171	0.029	0.049
Cr	0.004	0.008	0.007	0.007	0.035	0.007	0.007	0.006	0.037	0.013	0.001	0.011	0.006	0.053	0.008	0.015
Mg	11.381	11.479	11.276	11.120	11.272	11.258	11.375	11.502	11.119	11.378	11.128	11.503	11.502	11.115	11.331	11.317
Ca	0.009	0.009	0.006	0.000	0.002	0.002	0.007	0.013	0.000	0.004	0.001	0.009	0.013	0.001	0.005	0.005
Mn	0.014	0.006	0.003	0.003	0.005	0.002	0.002	0.015	0.008	0.002	0.003	0.000	0.015	0.009	0.006	0.006
Fe	0.262	0.314	0.350	0.390	0.246	0.336	0.367	0.270	0.251	0.263	0.373	0.378	0.270	0.213	0.309	0.299
Ni	0.021	0.034	0.042	0.042	0.037	0.042	0.044	0.019	0.027	0.042	0.038	0.054	0.019	0.024	0.036	0.036
Na	0.001	0.015	0.000	0.006	0.006	0.004	0.001	0.013	0.000	0.008	0.000	0.002	0.013	0.000	0.005	0.005
K	0.001	0.003	0.001	0.000	0.002	0.000	0.002	0.002	0.001	0.002	0.001	0.002	0.002	0.000	0.001	0.001

Table 3
Representative microprobe analyses of accessory chrome spinels in the serpentinites from Um Khariga

Sample no.	5U										3 U					
Spot no.	C_1*	R_1*	C_2	R_2	C_3	R_3	Single		Magnetite		C_1	R_1	C_2	R_2	Single	Magnetite
							1	2	1	2						
SiO_2	0.06	0.05	0.00	0.06	0.00	0.03	0.00	0.01	0.05	0.02	0.00	0.29	0.00	0.00	0.03	0.16
TiO_2	0.10	0.05	0.05	0.03	0.08	0.05	0.10	0.00	0.08	0.01	0.07	0.00	0.09	0.00	0.12	0.00
Al_2O_3	15.65	0.02	18.06	0.00	10.71	0.00	15.41	10.52	0.00	0.02	11.20	0.03	11.04	0.03	15.57	0.00
Cr_2O_3	52.32	2.18	49.51	3.30	56.13	2.49	50.53	53.70	0.03	0.01	55.75	2.64	55.48	1.62	49.45	0.00
Fe_2O_3	5.39	66.83	2.21	65.68	3.26	65.31	4.81	4.18	68.51	68.93	2.64	64.95	3.49	65.70	6.02	68.90
MgO	14.95	0.17	7.66	0.10	6.85	0.04	14.79	2.93	0.28	0.49	7.94	0.33	7.24	0.04	14.68	0.62
CaO	0.00	0.00	0.00	0.00	0.00	0.00	0.03	0.00	0.01	0.00	0.00	0.00	0.03	0.02	0.01	0.00
MnO	0.28	0.12	0.95	0.12	0.58	0.14	0.31	0.39	0.20	0.26	0.47	0.00	0.50	0.00	0.35	0.21
FeO	10.29	30.40	19.54	30.33	20.99	29.82	11.07	28.48	29.27	28.75	19.66	29.86	20.26	29.99	12.31	28.60
NiO	0.10	0.28	0.08	0.55	0.02	0.47	0.08	0.00	0.89	1.15	0.00	0.15	0.00	0.23	0.16	1.11
ZnO	0.00	0.07	0.30	0.00	0.35	0.12	0.09	0.21	0.08	0.06	0.38	0.07	0.28	0.05	0.00	0.12
Total	99.14	100.16	98.36	100.15	98.97	98.48	97.24	100.41	99.39	99.71	98.11	98.32	98.41	97.67	98.69	99.72
Structure formula based on 32 oxygens																
Si	0.014	0.015	0.000	0.019	0.000	0.010	0.000	0.002	0.016	0.007	0.000	0.091	0.000	0.000	0.008	0.048
Ti	0.019	0.011	0.010	0.006	0.016	0.012	0.020	0.000	0.018	0.003	0.014	0.000	0.019	0.000	0.022	0.000
Al	4.603	0.006	5.478	0.000	3.426	0.000	4.578	3.459	0.000	0.006	3.533	0.010	3.501	0.010	4.557	0.000
Cr	10.718	0.529	10.276	0.800	12.298	0.616	10.864	12.289	0.008	0.003	12.101	0.649	12.110	0.404	10.834	0.000
Fe^{3+}	0.637	15.434	0.233	15.169	0.257	15.356	0.533	0.249	15.951	15.978	0.348	15.227	0.366	15.587	0.571	15.940
Mg	5.561	0.077	3.336	0.046	2.814	0.021	5.556	1.219	0.129	0.227	3.165	0.154	2.905	0.017	5.508	0.286
Ca	0.000	0.000	0.001	0.000	0.000	0.000	0.008	0.000	0.002	0.000	0.001	0.000	0.008	0.008	0.002	0.000
Mn	0.059	0.032	0.207	0.030	0.133	0.038	0.067	0.092	0.053	0.067	0.106	0.000	0.114	0.000	0.074	0.055
Fe^{2+}	2.356	7.803	4.382	7.784	4.976	7.792	2.333	6.646	7.574	7.407	4.651	7.780	4.914	7.906	2.381	7.352
Ni	0.020	0.069	0.018	0.137	0.005	0.118	0.017	0.000	0.220	0.285	0.000	0.038	0.001	0.059	0.033	0.273
Zn	0.000	0.016	0.057	0.000	0.071	0.028	0.016	0.043	0.018	0.013	0.075	0.016	0.055	0.010	0.000	0.028
Cr#	0.70	0.99	0.65	1.00	0.78	1.00	0.70	0.78	1.00	0.38	0.77	0.98	0.78	0.98	0.70	
Mg#	0.70	0.01	0.43	0.01	0.36	0.00	0.70	0.16	0.02	0.03	0.40	0.02	0.37	0.00	0.70	

* C = Core; R = Rim (altered chrome spinel).

positions of serpentines, chrome spinels, olivine and magnesite were determined by electron microprobe techniques. The pyroxenes were not chemically analyzed because of the very small size of the fresh relicts.

5.1. Serpentine minerals

Representative chemical analyses of the serpentine minerals from Um Khariga and Gebel Ghadir serpentinites are represented in Tables 1, 2. Mean composition of Um Khariga serpentines is 42.78 ± 0.62 wt.% SiO_2, 41.14 ± 0.76 wt.% MgO, 0.23 ± 0.35 wt.% Al_2O_3, 1.99 ± 0.46 wt.% FeO and 0.02 ± 0.03 wt.% CaO. Meanwhile the mean composition of Gebel Ghadir serpentines is 43.19 ± 0.58 wt.% SiO_2, 40.95 ± 0.59 wt.% MgO, 0.22 ± 0.20 wt.% Al_2O_3, 1.95 ± 0.35 wt.% FeO and 0.03 ± 0.02 wt.% CaO. It is clear that the composition of the serpentine minerals in the two localities is similar. XRD charts, of serpentinites from both localities, revealed that antigorite is the main serpentine minerals with lesser amounts of chrysotile and lizardite. The abundance of antigorite indicates that the serpentinites were formed during prograde metamorphism (Deer et al., 1992).

5.2. Chrome spinel

Chromite is the only igneous mineral that retains most of its original chemistry in the serpentinized peridotites.

So, in the completely serpentinized ultramafic rocks containing no relicts of primary silicate minerals, the chemical composition of the unaltered accessory chromites has been widely recognized as a potentially important petrogenetic indicator (Irvine, 1965; Dick and Bullen, 1984; Jan and Windley, 1990; Arai, 1992; Sack and Ghiorso, 1991; Barnes and Roeder, 2001; Sobolev and Logvinova, 2005; Arif and Jan, 2006). The representative analyses of chrome spinel and its alteration products are shown in Tables 3, 4. Fresh chrome spinels (cores) show high Cr_2O_3 contents (49.45–56.13 wt.% in Um Khariga and 48.25–51.58 wt.% in Gebel Ghadir); the Cr# ranges from 0.65 to 0.78 and 0.61 to 0.63 in Um Khariga and Gebel Ghadir, respectively. On the other hand, the Mg# of the chrome spinels from Um Khariga serpentinites displays a wider range (0.16–0.76) than those from Gebel Ghadir (0.69–0.72).

Altered chrome spinels are represented by ferritchromite and Cr-magnetite; the former is the most common altered phase. The alteration of chromite to ferritchromite may have started during the late magmatic stage but it is mainly due to the much later serpentinization and tectonism (Khudeir et al., 1992). Ferritchromite is enriched in total iron and strongly depleted in Al_2O_3 and MgO. On the Cr–Al–Fe^{3+} diagram (Fig. 2a), the altered chrome spinels plot along the Cr–Fe^{3+} join, reflecting the loss in Al_2O_3 and Cr_2O_3 and increase in Fe_2O_3 due to alteration and metamorphism. Meanwhile, the fresh chrome spinels

Table 4
Representative microprobe analyses of accessory chrome spinels in the serpentinites from Gebel Ghadir

| Sample no.	6G					17 G						
Spot no.	Single	C_1*	R_1*	C_2	R_2	Single	C_1	R_1	C_2	R_2	Magentite	
											1	2
SiO_2	0.03	0.04	0.05	0.00	0.04	0.00	0.00	0.01	0.00	0.00	0.00	0.15
TiO_2	0.14	0.15	0.33	0.09	0.44	0.16	0.13	0.13	0.16	0.14	0.04	0.04
Al_2O_3	17.57	19.08	0.03	19.21	0.07	20.08	19.82	0.06	20.08	0.01	0.04	0.04
Cr_2O_3	50.27	49.94	21.68	51.58	26.31	48.25	49.67	2.45	49.57	20.33	0.03	0.02
Fe_2O_3	4.06	4.32	45.84	3.08	40.71	3.26	4.42	67.20	4.23	47.73	68.19	68.59
MgO	15.53	14.09	0.11	13.36	0.18	15.29	15.46	0.13	14.72	1.39	0.13	0.32
CaO	0.02	0.00	0.00	0.01	0.00	0.04	0.01	0.00	0.04	0.02	0.03	0.01
MnO	0.29	0.33	1.16	0.27	1.51	0.35	0.27	0.06	0.35	3.15	0.05	0.00
FeO	10.33	11.14	29.41	11.07	28.80	11.77	10.83	30.79	10.37	24.34	30.41	30.34
NiO	0.46	0.25	0.31	0.18	0.27	0.17	0.18	0.41	0.17	0.55	0.00	0.00
ZnO	0.21	0.00	0.00	0.03	0.13	0.10	0.00	0.04	0.10	0.68	0.00	0.11
Total	98.90	99.34	98.91	98.88	98.46	99.48	100.78	101.28	99.81	98.34	98.92	99.62
Structure formula based on 32 oxygens												
Si	0.007	0.011	0.016	0.000	0.012	0.000	0.001	0.004	0.000	0.000	0.000	0.048
Ti	0.026	0.028	0.077	0.016	0.101	0.031	0.024	0.029	0.031	0.033	0.010	0.010
Al	5.660	5.568	0.011	5.790	0.027	5.853	5.757	0.022	5.853	0.004	0.014	0.015
Cr	9.365	9.579	5.269	9.435	6.403	9.302	9.416	0.589	9.302	4.932	0.006	0.004
Fe^{3+}	0.935	0.805	10.605	0.755	9.428	0.806	0.797	15.348	0.806	11.022	15.967	15.908
Mg	5.497	5.570	0.049	5.624	0.082	5.425	5.683	0.057	5.425	0.635	0.063	0.146
Ca	0.004	0.001	0.000	0.001	0.001	0.010	0.002	0.000	0.010	0.006	0.010	0.002
Mn	0.060	0.069	0.303	0.057	0.395	0.074	0.056	0.015	0.074	0.819	0.013	0.000
Fe^{2+}	2.325	2.307	7.560	2.275	7.414	2.434	2.222	7.815	2.434	6.247	7.913	7.821
Ni	0.072	0.049	0.076	0.036	0.066	0.034	0.035	0.101	0.034	0.135	0.000	0.000
Zn	0.038	0.000	0.000	0.005	0.029	0.018	0.000	0.009	0.018	0.154	0.000	0.024
Cr#	0.62	0.63	1.00	0.62	1.00	0.61	0.62	0.96	0.61	1.00	0.32	0.22
Mg#	0.70	0.71	0.01	0.71	0.01	0.69	0.72	0.01	0.69	0.09	0.01	0.02

* C = Core; R = Rim (altered chrome spinel).
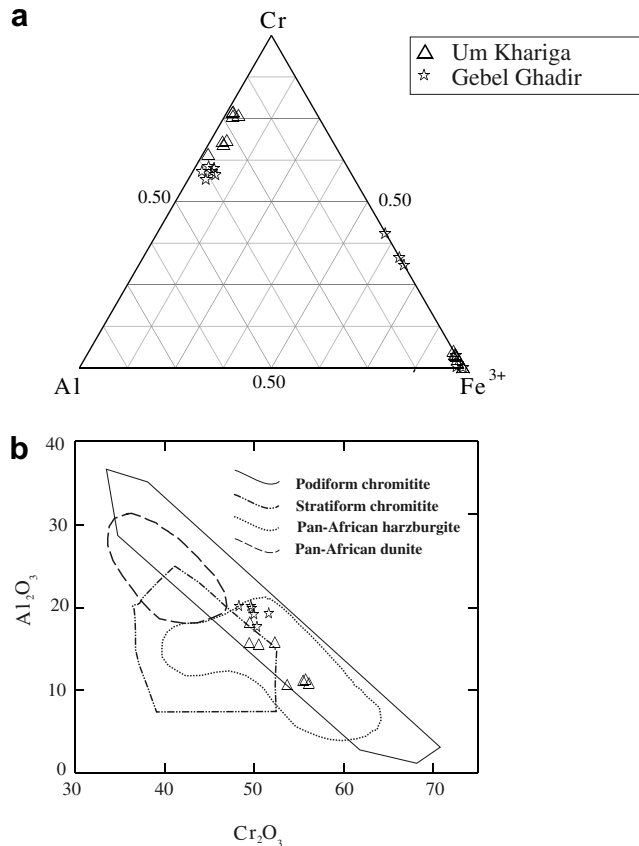
Fig. 2. (a) Cr–Al–Fe^{3+} plot of Um Khariga and Gebel Ghadir chrome spinels and their Al-poor alteration products. (b) Al$_2$O$_3$ versus Cr$_2$O$_3$ diagram for the accessory fresh chrome spinels (after Bonavia et al., 1993).

lie along the Cr–Al join. The analyzed chrome spinels have Fe^{3+} less than 0.1 and low TiO$_2$ contents which are similar to podiform chromite (Leblanc et al., 1980). Moreover, they are low in Al relative to Cr and are similar to ophiolitic podiform chromite associated with harzburgite (Fig. 2b).

5.3. Olivine

Fresh olivine relicts are recorded in many samples from Gebel Ghadir but were observed in few samples from Um Khariga serpentinites. Microprobe analyses of olivine relicts are represented in Table 5. Highly-strained olivines are analyzed from the two localities, while unstrained olivines are analyzed only from Gebel Ghadir. The highly-strained olivine gains have high Fo (89–96) content because they probably represent compositions of primary or mantle olivine, whereas the unstrained olivines have low Fo (84–85) content because they may have recrystallized during later metamorphic events. The limited composition range of the highly-strained olivine grains and their high Fo contents (>89) are comparable with olivines from Alpine peridotites (Coleman, 1977; Pearce et al., 1984).

5.4. Magnesite

Magnesite is an alteration product derived from magnesium-rich igneous and metamorphic rocks (Deer et al., 1992). The representative chemical analyses of magnesite of Gebel Ghadir are presented in Table 6. The studied magnesite occurs as sparse crystals or as cryptocrystalline veinlets. The former is rich in MgO and depleted in FeO than the latter. The sparse magnesite crystals may have been formed during serpentinization or somewhat later during low- to medium-grade metamorphism in the presence of CO$_2$. The monomineralic and cryptocrystalline character of the magnesite veinlets indicate precipitation from CO$_2$-rich solutions near surface conditions (Abu-Jaber and Kimberley, 1992). So, the magnesite veinlets might be ascribed to local shearing accompanied by hydrothermal solutions rich in CO$_2$.

The abundant of carbonates associated with the alteration of the ANS ophiolitic serpentinites suggests tremendous flux of CO$_2$-rich fluids from the mantle during Middle and Late Neoproterozoic time (Newton and Stern, 1990; Stern and Gwinn, 1990). In contrast, Surour and Arafa (1997) argued that the "ophicarbonates" of Wadi Ghadir ophiolites are reworked oceanic calcite grains recrystallized after the ophiolites were obducted. CO$_2$ may have been released from the sediments during regional metamorphism or brought from deeper levels (mantle origin). Decrease of partial pressure of carbon dioxide caused oversaturation of hydrothermal fluids resulting in the deposition of magnesite (Ghoneim et al., 2003). Similar magnesite veins in Gebel El-Rubshi and Gebel El-Maiyit in ED of Egypt formed after serpentinization near the earth surface (Salem et al., 1997; Ghoneim et al., 1999, 2003).

6. Geochemical characteristics

Representative chemical analyses of Um Khariga and Gebel Ghadir massive serpentinites are given in Tables 7, 8. All the analyzed samples have high LOI values (11.85–15.99 wt.%) which indicate the hydrated nature of these rocks. Um Khariga serpentinites show limited variation in their compositions. They contain 37.45–38.53 wt.% SiO$_2$, 37.49–38.55 wt.% MgO, 0.40–0.56 wt.% Al$_2$O$_3$ and 7.52–7.99 wt.% total iron as Fe$_2$O$_3$; Cr and Ni contents are high (2019–2953 ppm and 1765–2248 ppm, respectively), whereas Co ranges from 95 to 105 ppm. The serpentinites of Gebel Ghadir show a wide variation in SiO$_2$ (36.86–41.60 wt.%), MgO (34.70–40.06 wt.%), CaO (0.01-0.59 wt.%), Fe$_2$O$_3$ (6.66–8.74 wt.%), Cr (1945–3107), and Ni (1133–3000 ppm) contents. Low abundances of Al$_2$O$_3$ (<1.08 wt.%) and CaO (<0.68 wt.%) in the serpentinites are consistent with the absence of clinopyroxene in peridotite (Dick and Bullen, 1984).

Serpentinites show high Mg# (100 molar Mg/Mg + Fe), which ranges from 90.37 to 91.04 (mean = 90.68 ± 0.19) in Um Khariga and from 89.06 to 92.0 (mean = 90.75 ± 0.74) in Gebel Ghadir. Geochemical data indicate that, except

Table 5
Representative microprobe analyses of olivine from Um Khariga and Gebel Ghadir

Locality	Um Khariga					Gebel Ghadir												
Sample no.	5U[*]					9Ga						9Gb				13G[*]		
Spot No	1	2	3	4	5	1	2	3	4	5	6	1	2	3	4	1	2	3
SiO_2	40.68	40.88	40.90	41.46	40.94	39.63	39.70	39.46	39.53	39.56	39.88	39.36	39.45	39.58	39.98	42.06	41.88	40.97
TiO_2	0.00	0.00	0.00	0.00	0.00	0.02	0.01	0.01	0.05	0.00	0.00	0.00	0.02	0.00	0.00	0.02	0.00	0.02
Al_2O_3	0.02	0.03	0.02	0.04	0.00	0.05	0.0118	0.00	0.04	0.16	0.11	0.00	0.00	0.00	0.00	0.00	0.02	0.10
Cr_2O_3	0.02	0.05	0.02	0.01	0.03	0.03	0.05	0.09	0.02	0.15	0.05	0.01	0.00	0.06	0.00	0.00	0.03	0.00
MgO	49.20	49.48	49.40	51.52	49.67	44.67	44.50	44.23	44.17	44.08	44.44	44.52	44.35	45.06	45.36	54.06	53.26	44.81
CaO	0.06	0.06	0.06	0.00	0.07	0.01	0.02	0.01	0.00	0.00	0.02	0.01	0.00	0.01	0.00	0.03	0.04	0.01
MnO	0.13	0.10	0.14	0.12	0.17	0.12	0.08	0.10	0.08	0.05	0.11	0.08	0.07	0.07	0.11	0.12	0.56	0.17
FeO	8.67	8.71	8.77	6.72	8.77	14.82	14.67	15.14	14.82	13.80	14.15	15.11	14.48	14.82	14.66	3.69	3.84	10.11
NiO	0.35	0.40	0.38	0.22	0.45	0.15	0.15	0.06	0.13	0.24	0.18	0.11	0.22	0.25	0.20	0.15	0.14	0.15
Total	99.13	99.71	99.68	100.09	100.12	99.50	99.18	99.11	98.82	98.04	98.94	99.20	98.58	99.83	100.31	100.14	99.76	96.33
Structure formula based on 4 oxygens																		
Si	1.002	1.001	1.002	1.001	0.999	0.999	1.003	1.000	1.003	1.008	1.007	0.997	1.003	0.995	0.999	1.001	1.003	1.040
Ti	0.000	0.000	0.000	0.000	0.000	0.000	0.000	0.000	0.001	0.000	0.000	0.000	0.000	0.000	0.000	0.000	0.000	0.000
Al	0.001	0.001	0.001	0.001	0.000	0.002	0.000	0.000	0.001	0.005	0.003	0.000	0.000	0.000	0.000	0.000	0.001	0.003
Cr	0.000	0.001	0.000	0.000	0.001	0.001	0.001	0.002	0.000	0.003	0.001	0.000	0.000	0.001	0.000	0.000	0.001	0.003
Mg	1.806	1.806	1.804	1.854	1.807	1.679	1.676	1.671	1.671	1.674	1.673	1.681	1.680	1.689	1.689	1.918	1.901	1.695
Ca	0.002	0.002	0.002	0.000	0.002	0.000	0.001	0.000	0.000	0.000	0.001	0.000	0.000	0.000	0.000	0.001	0.001	0.000
Mn	0.003	0.002	0.003	0.002	0.004	0.003	0.002	0.002	0.002	0.001	0.002	0.002	0.002	0.001	0.002	0.002	0.011	0.004
Fe	0.179	0.178	0.180	0.136	0.179	0.312	0.310	0.321	0.315	0.294	0.299	0.320	0.308	0.312	0.306	0.073	0.077	0.215
Ni	0.007	0.008	0.008	0.004	0.009	0.004	0.003	0.001	0.003	0.005	0.004	0.002	0.005	0.005	0.004	0.003	0.003	0.003
Fo	0.91	0.91	0.91	0.93	0.91	0.84	0.84	0.84	0.84	0.85	0.85	0.84	0.85	0.84	0.85	0.96	0.96	0.89

[*] Strained olivine grains.

Table 6
Representative microprobe analyses of magnesite from Gebel Ghadir

Sample	Disseminated		Veins	
	6G		192	
SiO_2	1.66	0.05	0.02	0.00
TiO_2	0.00	0.00	0.00	0.00
Al_2O_3	0.00	0.02	0.00	0.00
Cr_2O_3	0.02	0.00	0.21	0.01
MgO	47.49	48.80	42.33	45.10
CaO	0.05	0.10	0.18	0.17
MnO	0.73	0.11	0.23	0.09
FeO	1.65	1.35	8.30	5.47
NiO	0.00	0.12	0.06	0.06
Na_2O	0.00	0.00	0.04	0.00
K_2O	0.00	0.01	0.00	0.00
Total	51.60	50.55	51.37	50.90
Si	0.7	0.02	0.01	0
Ti	0	0	0	0
Al	0	0.01	0	0
Cr	0.01	0	0.08	0
Mg	29.73	31.33	28.52	29.83
Ca	0.02	0.05	0.09	0.08
Mn	0.26	0.04	0.09	0.03
Fe^{2+}	0.58	0.49	3.14	2.03
Ni	0	0.04	0.02	0.02
Na	0	0	0.04	0
K	0	0	0	0

for addition of water, no significant addition or removal of elements occurred during the serpentinization processes. So, it is permissible to compare the studied serpentinites with peridotites from modern tectonic settings. Serpentinites of Um Khariga and Gebel Ghadir have very low abundances of Al_2O_3 (0.32–1.08 wt.%) similar to the fore-arc peridotites and Egyptian serpentinized peridotites (Fig. 3a). Moreover, on the Al_2O_3 vs. CaO diagram (Fig. 3b), serpentinites are depleted in Al_2O_3 and CaO similar to fore-arc peridotites. The high Mg# accompanied by high contents of Ni, Cr and Co and depletion in the incompatible elements reflect the depleted and highly refractory nature of the parent rocks (Roberts, 1992). Moreover, the high Cr# of the disseminated chrome spinels combined with the high contents of Ni, Cr and Co in the bulk serpentinites suggest high degree of partial melting (Dick and Bullen, 1984; Arai, 1994; Ishiwatari et al., 2003).

7. Discussion

The tectonic setting of Egyptian ophiolites is still a subject of debate. Some of the earlier authors suggest a mid-ocean ridge setting for the Egyptian ophiolites (Shackleton et al., 1980; Zimmer, 1989; Zimmer et al., 1995). Recent geochemical studies of Egyptian ophiolites recognize their transitional geochemical character, which lie between those of island arcs and MORB and on this basis, a back-arc environment of formation is later inferred (Abu El Ela, 1990; Khudeir and Asran, 1992; El-Sayed et al., 1999; Ahmed et al., 2001, 2006; Abdel Aal et al., 2003; El Bahariya and Arai, 2003; Farahat et al., 2004). Azer and Stern

(2007) attributed the transitional geochemical characters between island arcs and MORB for the Egyptian ophiolites to the transfer of LILE and volatile-rich components from the subduction zone into the overlying mantle wedge. Interpreting the tectonic setting of the Neoproterozoic ophiolitic rocks based on their major and trace element compositions encounters difficulties due to the effects of fractional crystallization and alteration. As a result, distinguishing fore-arc and back-arc ophiolites can yield equivocal results. Recently, the microprobe analyses of primary spinels and mafic minerals are used to infer the tectonic setting for the ANS ophiolites (Stern et al., 2004; Azer and Stern, 2007). ANS ophiolitic ultramafic rocks contain spinels and olivines comparable to those of modern fore-arc environments.

The geochemical and mineralogical characteristics of Um Khariga and Gebel Ghadir serpentinites indicate that they are derived from harzburgite and minor dunite. So, the ultramafic protoliths of these serpentinites are chemically akin to the depleted mantle sequences of SSZ ophiolites associated with island arcs. The depleted nature of the studied serpentinites is confirmed by using the Cr# vs. TiO_2 diagram for the fresh chrome spinels (Fig. 4). The highly depleted peridotite with high Cr# (>0.7) spinels can be produced in the mantle wedge beneath arcs or in plume-related within-plate mantle (Pearce et al., 1984; Arai, 1994; Ishiwatari et al., 2003). The TiO_2 content of spinel in the magma varies depending on the tectonic site of magma generation; TiO_2 is low in arc magma, intermediate in MORB and high in the intraplate magma (Arai, 1992). So, the high Cr# and low TiO_2 spinel as well as their depleted nature suggest an origin from a mantle wedge or a sub-arc mantle.

Spinels retain most of their original chemistry in ophiolites and serve as robust petrogenetic indicators. In the present study, we used compositions of fresh spinel cores to infer the petrogenesis of serpentinites because they are least likely to have been affected by regional metamorphism. Fore-arc peridotites contain accessory spinels with high Cr# (up to 0.80; Ohara and Ishii, 1998; Stern et al., 2004). In contrast, back-arc basin peridotites contain accessory chromite with Cr# ⩽ 0.55 similar to those of MOR peridotites (Ohara et al., 2002; Ohara, 2006). Mid-ocean ridge peridotite spinels rarely have Cr# greater than 0.55 which is the composition of chromite in equilibrium with mantle pyroxene at the point where diopside disappears from the mantle residue (Dick and Fisher, 1984). Adopting the above criteria, the chrome spinels of Um Khariga and Gebel Ghadir serpentinites are very similar to those in peridotites from modern fore-arcs. Moreover, on the Cr# vs. Mg# diagram (Fig. 5), fresh chrome spinels are plotted mainly within the fore-arc field. The high Cr# of the primary chrome spinels correlates positively with the degree of partial melting, as chrome spinels become richer in Cr with increasing degrees of depletion (Irvine, 1965; Dick and Bullen, 1984).

The relics of primary olivines can provide insights into the tectonic setting at which the ultramafic protoliths were

Table 7
Chemical analyses of massive serpentinites from Um Khariga area

Sample no.	1U	2U	3U	4U	5U	6U	7U	8U	9U	10U	11U	12U	13U	14U	15U	17U	18U	19U	20U	21U	22U	23U	24U
SiO_2	38.32	38.29	37.98	37.92	38.27	37.87	38.41	38.38	37.45	37.87	37.85	38.12	37.69	38.31	38.31	37.97	37.96	38.53	37.97	38.43	38.46	37.55	37.77
TiO_2	0.01	0.01	0.01	0.01	0.01	0.01	0.01	0.01	0.01	0.01	0.01	0.01	0.01	0.01	0.01	0.01	0.01	0.01	0.01	0.01	0.01	0.01	0.01
Al_2O_3	0.50	0.40	0.40	0.48	0.55	0.45	0.43	0.42	0.43	0.54	0.56	0.40	0.41	0.49	0.55	0.52	0.41	0.42	0.45	0.45	0.51	0.43	0.47
Fe_2O_3 [*]	7.54	7.67	7.97	7.95	7.87	7.57	7.96	7.91	7.86	7.77	7.52	7.71	7.94	7.96	7.86	7.56	7.76	7.99	7.92	7.77	7.56	7.79	7.92
MnO	0.11	0.11	0.11	0.10	0.07	0.11	0.10	0.11	0.10	0.11	0.11	0.11	0.11	0.10	0.11	0.11	0.11	0.10	0.10	0.09	0.11	0.11	0.11
MgO	37.92	38.42	38.45	37.97	37.87	38.12	37.49	37.92	38.39	37.93	37.97	38.27	37.89	37.90	38.51	38.55	37.98	37.89	38.32	37.59	37.82	38.38	37.98
CaO	0.46	0.33	0.25	0.59	0.07	0.43	0.31	0.24	0.53	0.27	0.47	0.32	0.26	0.58	0.08	0.46	0.34	0.24	0.56	0.08	0.47	0.35	0.24
Na_2O	0.18	0.16	0.08	0.09	0.04	0.13	0.14	0.01	0.07	0.04	0.17	0.15	0.08	0.09	0.05	0.18	0.17	0.08	0.11	0.06	0.19	0.18	0.12
K_2O	0.01	0.01	0.01	0.01	0.01	0.01	0.01	0.01	0.01	0.01	0.01	0.01	0.01	0.01	0.01	0.01	0.01	0.01	0.01	0.01	0.01	0.01	0.01
P_2O_5	0.00	0.01	0.01	0.00	0.01	0.00	0.01	0.00	0.01	0.01	0.01	0.01	0.01	0.00	0.01	0.00	0.01	0.01	0.00	0.01	0.00	0.01	0.00
LOI	14.31	14.25	14.55	14.34	15.21	14.43	14.20	14.45	14.36	14.54	14.34	14.27	14.68	14.44	14.30	14.41	14.53	14.38	14.41	15.24	14.40	14.87	14.59
Total	99.36	99.65	99.81	99.47	99.98	99.13	99.07	99.46	99.22	99.09	99.01	99.37	99.08	99.90	99.79	99.78	99.28	99.65	99.87	99.74	99.54	99.68	99.22
Mg#	90.93	90.89	90.58	90.49	90.55	90.94	90.37	90.52	90.68	90.68	90.96	90.82	90.48	90.46	90.71	91.04	90.70	90.43	90.60	90.60	90.88	90.75	90.52
Trace elements (ppm)																							
Ba	<10	<10	<10	<10	<10	<10	<10	<10	<10	<10	<10	<10	<10	<10	<10	<10	<10	<10	<10	<10	<10	<10	<10
Co	99	99	105	96	95	98	100	103	97	98	101	99	104	97	97	99	96	100	98	95	93	99	103
Cr	2227	2019	2943	2639	2349	2274	2063	2932	2649	2359	2237	2129	2933	2629	2347	2247	2239	2947	2645	2419	2239	2079	2953
Cu	<10	<10	<10	<10	<10	<10	<10	<10	<10	<10	<10	<10	<10	<10	<10	<10	<10	<10	<10	<10	<10	<10	<10
Nb	<2	<2	<2	<2	<2	<2	<2	<2	<2	<2	<2	<2	<2	<2	<2	<2	<2	<2	<2	<2	<2	<2	<2
Ni	2223	2214	2247	2166	1765	2233	2216	2248	2167	1769	2233	2224	2247	2176	1769	2225	2224	2217	2176	1785	2229	2218	2240
Pb	<3	<3	6	<3	4	<3	<3	6	<3	4	<3	<3	6	<3	4	<3	<3	6	<3	4	<3	<3	6
Rb	<2	<2	<2	<2	<2	<2	<2	<2	<2	<2	<2	<2	<2	<2	<2	<2	<2	<2	<2	<2	<2	<2	<2
Sr	6	9	7	16	12	8	9	10	15	12	9	14	8	13	12	7	16	12	15	11	8	13	7
V	33	37	33	44	28	34	37	35	42	28	31	37	34	43	29	33	36	32	42	28	34	38	32
Y	3	2	<2	3	<2	3	3	2	3	2	3	2	<2	3	2	3	2	<2	2	<2	2	3	<2
Zn	34	35	41	36	35	35	36	40	35	36	33	35	39	37	35	36	35	41	34	41	35	36	41
Zr	10	10	8	12	9	11	10	12	11	9	9	10	8	9	12	10	11	8	11	9	12	10	8

[*] Total iron determined as Fe_2O_3.

Table 8
Chemical analyses of massive serpentinites from Gebel Ghadir area

Sample no.	6G	7G	9Ga	9Gb	10G	11G	13G	14G	15G	16G	17G	25G
SiO_2	40.65	40.82	41.50	40.80	36.86	39.90	41.60	39.40	40.60	38.67	37.96	37.86
TiO_2	0.01	0.01	0.02	0.01	0.01	0.01	0.01	0.01	0.06	0.01	0.01	0.01
Al_2O_3	0.65	0.72	1.08	0.74	0.32	0.76	0.73	0.68	0.86	0.59	0.67	0.52
Fe_2O_3 [*]	7.86	7.77	7.34	7.56	7.96	7.43	7.12	6.66	8.74	6.96	7.09	7.96
MnO	0.05	0.04	0.14	0.11	0.19	0.06	0.10	0.12	0.14	0.09	0.09	0.10
MgO	35.87	35.93	38.01	37.35	40.06	35.85	36.88	38.45	35.70	36.64	36.78	38.17
CaO	0.02	0.17	0.06	0.01	0.20	0.04	0.27	0.05	0.59	0.68	0.30	0.58
Na_2O	0.05	0.04	0.04	0.04	0.04	0.06	0.03	0.04	0.03	0.05	0.05	0.11
K_2O	0.01	0.01	0.01	0.01	0.01	0.01	0.01	0.01	0.01	0.01	0.01	0.01
P_2O_5	0.01	0.01	0.01	0.01	0.01	0.01	0.00	0.00	0.01	0.01	0.00	0.00
LOI	13.75	13.65	11.85	12.65	14.32	14.25	12.43	13.62	12.89	15.20	15.99	14.36
Total	98.92	99.17	100.05	99.29	99.98	98.37	99.18	99.04	99.63	98.90	98.95	99.69
Mg#	90.09	90.21	91.16	90.78	90.93	90.58	91.17	92.00	89.06	91.30	91.18	90.52
Trace elements (ppm)												
Ba	<10	<10	<10	<10	<10	<10	<10	<10	<10	<10	<10	<10
Co	142	95	96	113	95	92	95	88	127	96	93	96
Cr	3000	1945	2403	2494	2603	2667	2332	2290	2599	2672	2708	2657
Cu	<10	<10	<10	<10	<10	<10	<10	<10	<10	<10	<10	<10
Nb	<2	<2	<2	<2	<2	<2	<2	<2	<2	<2	<2	<2
Ni	2397	1635	2437	2156	3330	1632	2125	2301	1133	2003	1893	2165
Pb	<3	4	<3	6	<3	<3	<3	<3	<3	3	7	<3
Rb	<2	<2	<2	<2	<2	<2	<2	<2	<2	<2	<2	<2
Sr	3	4	7	3	13	5	4	4	6	5	11	16
V	35	31	55	48	26	42	27	28	70	34	40	41
Y	<2	<2	3	<2	3	<2	<2	<2	<2	<2	<2	3
Zn	45	38	53	46	33	39	41	38	35	34	49	36
Zr	9	10	10	8	10	10	9	7	10	9	10	12

[*] Total iron determined as Fe_2O_3.
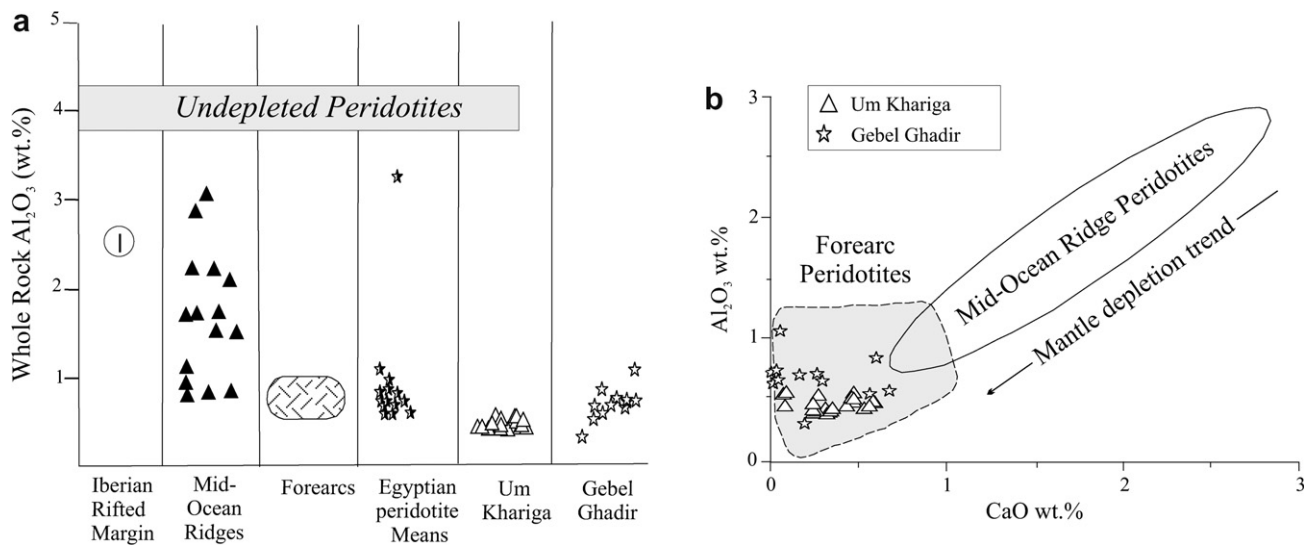
Fig. 3. (a) Whole-rock Al_2O_3 content in Um Khariga and Gebel Ghadir serpentinites and in other Egyptian Neoproterozoic serpentinized peridotites compared with peridotites from other tectonic settings (modified after Bonatti and Michael, 1989). The means of the different localities in the Eastern Desert of Egypt are adopted from Azer and Stern (2007). (b) Al_2O_3 vs. CaO diagram (after Ishii et al., 1992) for comparing Um Khariga and Gebel Ghadir serpentinites with peridotites from other tectonic settings.

formed, viz. supra-subduction setting or mid-ocean ridge setting (Parkinson and Pearce, 1998). In the present study, only the compositions of the highly-strained olivine grains were used to infer the tectonic setting of their parent rocks, because they probably represent the compositions

of primary or mantle olivine. The Mg-rich nature of the highly-strained olivines (Fo > 89) indicate that they were residual after extensive melting similar to fore-arc peridotites (Coish and Gardner, 2004). In the fore-arc environment, depleted mantle is available as well as water to
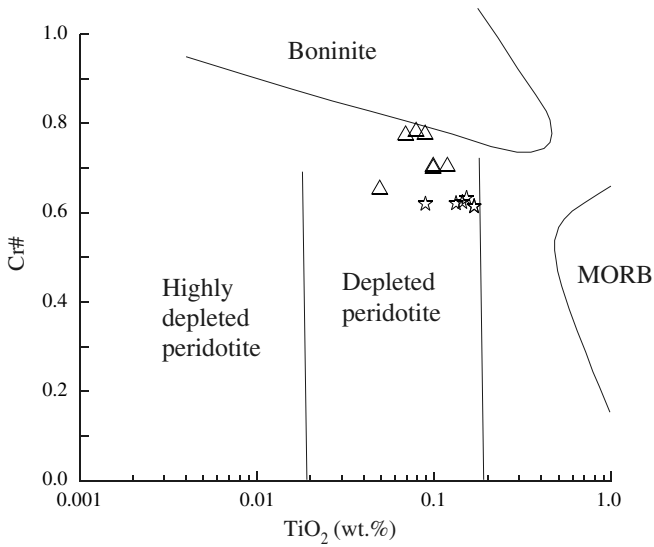
Fig. 4. Cr# vs. TiO$_2$ diagram for the analyzed accessory fresh chrome spinels (fields after Dick and Bullen, 1984; Arai, 1992; Jan and Windley, 1990).
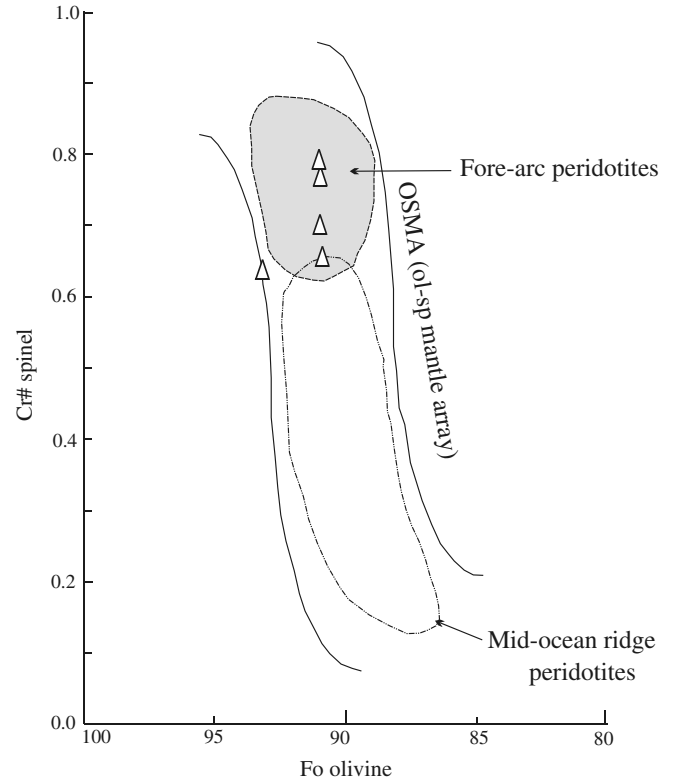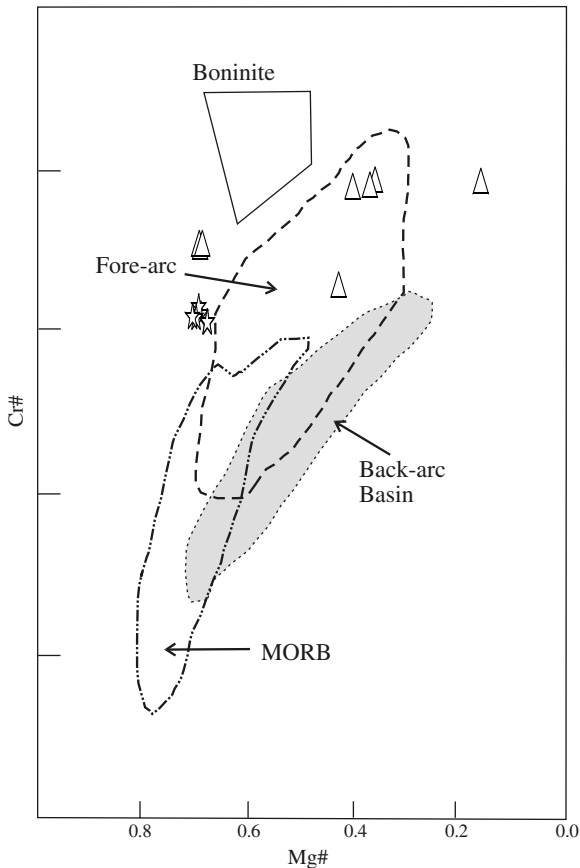

Fig. 5. Cr# vs. Mg# diagram for the fresh chrome spinels (after Stern et al., 2004). The field boundaries are from Dick and Bullen (1984), Bloomer et al. (1995) and Ohara et al. (2002).

Fig. 6. Cr# in spinels against Fo in coexisting olivine in Um Khariga serpentinites (fields after Arai, 1994).

et al., 2000). So, the resulting harzburgite and dunite have very high Mg-olivine and high Cr-spinel not found in the peridotites from any other modern tectonic environment. Fo contents in the strained olivines are greater than 0.88 similar to the ANS ophiolites formed in fore-arc basins (Stern et al., 2004). Moreover, the chemical analyses of coexisting olivine and chrome spinel in the Um Khariga serpentinites support a fore-arc setting (Fig. 6).

Boninitic affinities of some ED ophiolitic rocks have been recognized (El-Sayed et al., 1999; Abdel Aal et al., 2003) which support the fore-arc setting for these rocks. Since the beginning of the Phanerozoic boninites are restricted to fore-arc environments (Hawkins et al., 1984; Murton, 1989; Johnson and Fryer, 1990; Stern and Bloomer, 1992; Bédard, 1999; Beccaluva et al., 2004).

8. Summary

Before serpentinization, the Um Khariga and Gebel Ghadir peridotites were harzburgite and dunite due to the prevalence of bastite and mesh texture, respectively. Despite deformation and metamorphism, remnant olivine and spinel grains occur; their compositions provided important clues to their tectonic environments. A noteworthy feature in the present serpentinized peridotites is the presence of olivine in two textural types: (a) highly-strained olivine grains with kink bands, as in the deformed mantle tectonites from ophiolites, and (b) non-strained grains.

reduce its high melting temperature. Therefore, hydrous partial melting of depleted mantle arc thoeliite or boninite leaves behind a residue of very depleted peridotite (Pearce
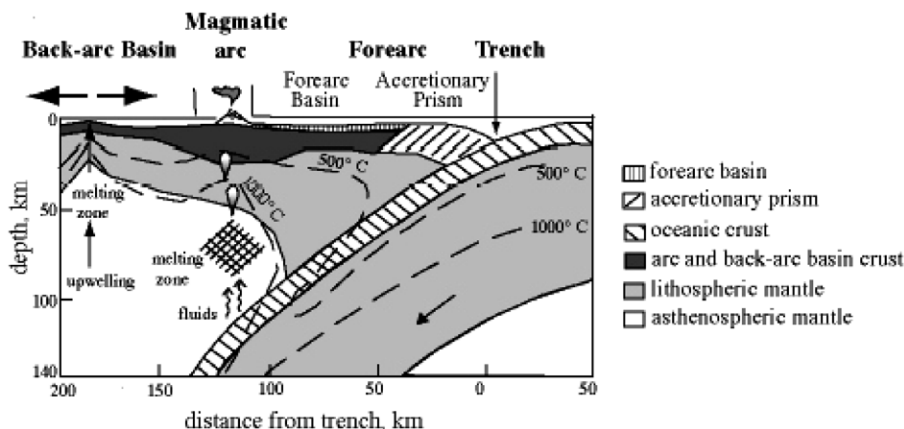
Fig. 7. Cartoon showing the tectonic setting of Um Khariga and Gebel Ghadir serpentinized peridotites in the fore-arc environment (adopted from Azer and Stern, 2007).

The latter was observed only in the Gebel Ghadir serpentinites and may represent recrystallized crystals during later thermal metamorphic events due to the intrusion of granite.

The mineral and whole-rock chemical data reported here indicate that the serpentinized peridotites of Um Khariga and Gebel Ghadir were refractory mantle residues. As the mantle partially melts, the olivine left in the residue became more Mg-rich and the spinel more Cr-rich as Fe and Al are partitioned into the early melts. High Cr/(Cr + Al) in chrome spinel and high Mg/(Mg + Fe) in olivine indicate that the serpentinites formed as highly-depleted mantle residues. The mineralogical and geochemical compositions of the serpentinized peridotites of Um Khariga and Gebel Ghadir are similar to those in peridotites from fore-arc regions of subduction zone. Therefore, the studied serpentinized peridotites represent a fragment of oceanic lithosphere that formed in a fore-arc environment (Fig. 7); that is, they belong to an ophiolitic mantle sequence formed in a supra-subduction zone. The present results are comparable with those of ANS ophiolites (Stern et al., 2004; Azer and Stern, 2007).

References

Abdel Aal, A.Y., Farahat, E.S., Hoinken, G., El-Mahalawi, M.M., 2003. Ophiolites from the Egyptian Shield: A case for a possible inter-arc origin. Mitt. Osterr. Ges. 148, 81–83.

Abu El Ela, F.F., 1990. Supra-subduction zone ophiolite of Qift-Quseir Road, Eastern Desert, Egypt. Bulletin Faculty of Science, Assiut University 19, pp. 51–70.

Abu-Jaber, N.S., Kimberley, M.M., 1992. Origin of ultramafic-hosted vein magnesite deposits. Ore Geology Review 7, 155–191.

Ahmed, A.A. 2005. The status of uncertain ''ophiolites'' in the Eastern Desert of Egypt. In: 1st Symposium on the classification of the basement complex of Egypt, pp. 52–61.

Ahmed, A.H., Aria, S., Attia, A.K., 2001. Petrological characteristics of podiform chromitites and associated peridotites of Pan-African complexes of Egypt. Mineralium Deposita 36, 72–84.

Ahmed, A.H., Hanghøj, K., Kelemen, P.B., Hart, S.R., Arai, S., 2006. Osmium isotope systematics of the Proterozoic and Phanerozoic ophiolitic chromitites: In situ ion probe analysis of primary Os-rich PGM. Earth and Planetary Science Letters 245, 777–791.

Akaad, M.K., Abu El Ela, A.M., El Kamhoshy, H.I., 1994. Geology of the region west of Mersa Alam, Eastern Desert, Egypt. Annals of the Geological Survey of Egypt 24, 1–18.

Arai, S., 1992. Chemistry of chromain spinel in volcanic rocks as a potential guide to magma chemistry. Mineralogical Magazine 56, 173–184.

Arai, S., 1994. Compositional variation of olivine-chromain spinel in Mg-rich magmas as a guide to their residual spinel peridotites. Journal of Volcanology and Geothermal Research 59, 279–294.

Arif, M., Jan, M.Q., 2006. Petrotectonic significance of the chemistry of chromite in the ultramafic-mafic complexes of Pakistan. Journal of Asian Earth Sciences 27, 628–646.

Azer, M.K., Khalil, A.E.S., 2005. Petrological and mineralogical studies of Pan-African serpentinites at Bir Al-Edeid area, Central Eastern Desert, Egypt. Journal of African Earth Sciences 43, 525–536.

Azer, M.K., Stern, R.J., 2007. Neoproterozoic (835-720 Ma) serpentinites in the Eastern Desert, Egypt: Fragments of Fore-arc mantle. The Journal of Geology 15, 457–472.

Barnes, S.J., Roeder, P.L., 2001. The range of spinel composition in terrestrial mafic ultramafic rocks. Journal of Petrology 42, 2279–2302.

Beccaluva, L., Coltori, M., Giunta, G., Siena, F., 2004. Tethyan vs. Cordilleran ophiolites: a reappraisal of distinctive tectono-magmatic features of supra-subduction complexes in relation to subduction mode. Tectonophysics 393, 163–174.

Bédard, J.H., 1999. Petrogensis of boninites from the Betts Cove ophiolite, Newfoundland, Canada: identification of subducted source components. Journal of Petrology 40, 1853–1889.

Bloomer, S.H., Taylor, B., MacLeod, C.J., Stern, R.J., Fryer, P., Hawkins, J.W., Johnson, L., 1995. Early arc volcanism and ophiolite problem: A perspective from drilling in the Western Pacific. In: Taylor, B., Natland, J. (Eds.), Active Margins and Marginal Basins of the Western Pacific, Geophysical Monograph, Vol. 88. American Geophysical Union, Washington, DC, pp. 1–30.

Bonatti, E., Michael, P.J., 1989. Mantle peridotites from continental rifts to oceanic basins to subduction zones. Earth and Planetary Science Letters 91, 297–311.

Bonavia, F.F., Diella, V., Ferrario, A., 1993. Precambrian podiform chromitites from Kenticha Hill, southern Ethiopia. Economic Geology 88, 198–202.

Coish, R.A., Gardner, P., 2004. Suprasubduction-zone peridotite in the northern USA Appalachians: evidence from mineral composition. Mineralogical Magazine 68, 699–708.

Coleman, R.G., 1977. Ophiolites. Springer-Verlag, Berlin, 229pp.

Deer, W.A., Howie, R.A., Zussman, J., 1992. An introduction to the rock forming minerals. Second ed., Longman Scientific and Technical, London, pp. 696.

Dick, H.B., Fisher, R.L., 1984. Mineralogic studies of the residues of mantle melting; abyssal and alpine-type peridotites. In: Kornprobst, J. (Ed.), Kimberlites; II, The Mantle and Crust-mantle Relationships, Vol. 11B. Elsevier, Amsterdam, pp. 295–308.

Dick, H.B., Bullen, T., 1984. Chromian spinel as a petrogenetic indicator in abyssal and Alpine-type peridotites and spatially associated lavas. Contribution to Mineralogy and Petrology 86, 54–76.

El Bahariya, G.A., Arai, S., 2003. Petrology and origin of Pan-African serpentinites with particular reference to chromian spinel compositions, Eastern Desert, Egypt: Implication for supra-subduction zone ophiolite. In: 3rd International Conference on the Geology of Africa, Assiut University, Egypt, pp. 371–388.

El Bayoumi, R.M., 1980. Ophiolites and associated rocks of Gebel Ghadir area, east of Gabal Zabara, Eastern Desert, Egypt. Ph.D. Thesis, Cairo University, Egypt, 171 pp.

El Bayoumi, R.M., 1983. Ophiolites and mélange complex of Wadi Ghadir area, Eastern Desert, Egypt. Bulletin of Faculty of Science, King Abdul Aziz University 6, pp. 329–342.

El Gaby, S., 2005. Integrated evolution and rock classification of the Pan-African belt in Egypt. 1st Symposium on the classification of the basement complex of Egypt, pp. 1–9.

El Gaby, S., List, F.K., Tehrani, R., 1988. Geology, evolution and metallogenesis of the Pan-African Belt in Egypt. In: El Gaby, S., Greiling, R.O. (Eds.), The Pan-African Belt of northeast Africa and adjacent areas. Braunschweig Viewig, pp. 17–68.

El Sharkawy, M.A., El Bayoumi, R.M., 1979. The ophiolites of Wadi Ghadir area, Eastern Desert, Egypt. Annals of the Geological Survey of Egypt 9, 125–135.

El-Sayed, M.M., Furnes, H., Mohamed, F.H., 1999. Geochemical constraints on the tectonomagmatic evolution of the late Precambrian Fawakhir ophiolite, Central Eastern Desert, Egypt. Journal of African Earth Sciences 29, 515–533.

Farahat, E.S., El Mahalawi, M.M., Hoinkes, G., 2004. Continental back-arc basin origin of some ophiolites from the Eastern Desert of Egypt. Mineralogy and Petrology 82, 81–104.

Ghoneim, M.F., Salem, I.A., Hamdy, M.M., 1999. On the petrogenesis of magnesite from Gebel El-Maiyit, Central Eastern Desert, Egypt. In: The Fourth International Conference on Geology of the Arab World, Cairo University 1, pp. 575–593.

Ghoneim, M.F., Salem, I.A., Hamdy, M.M., 2003. Origin of magnesite veins in serpentinites from Mount El-Rubshi and Mount El-Maiyit, Eastern Desert, Egypt. Archiwum Mineralogiczne T, LIV, 41–63.

Hawkins, J.W., Bloomer, S.H., Evans, C.A., Melchior, J.T., 1984. Evolution of intra-oceanic arc-trench system. Tectonophysics 102, 175–205.

Irvine, T.N., 1965. Chrome spinel as a petrogenetic indicator. Part I. Theory. Canadian Journal of Earth Sciences 2, 648–671.

Ishii, T., Robinson, P.T., Maekawa, H., Fiske, R., 1992. Petrological studies of peridotites from diapiric Serpentinite Seamounts in the Izu-Ogasawara-Mariana forearc, leg 125. In: J. Pearce, L.B. Stokking, et al. (Eds.), Proceedings of the Ocean Drilling Project, Leg 125, Scientific Results (College Station), pp. 445–485.

Ishiwatari, A., Sokolov, S.D., Vysotskiy, S.V., 2003. Petrological diversity and origin of ophiolites in Japan and Far East Russia with emphasis on depleted harzburgite. In: Dilek, Y., Robinson, P.T. (Eds.), Ophiolites in Earth History. Special Publication, Geological Society of London 128, pp. 597–617.

Jan, M.Q., Windley, B.F., 1990. Chromian spinel-silicate chemistry in ultramafic rocks of the Jijal complex, Northwestern Pakistan. Journal of Petrology 31, 667–715.

Johnson, L.E., Fryer, P., 1990. The first evidence for MORB-like lavas from the outer Mariana forearc: geochemistry, petrography and tectonic implications. Earth and Planetary Science Letters 100, 304–316.

Khalil, A.E.S., 2000. Petrological and geochemical studies on the serpentinites of Umm Saneyat, El Deigheimi and El Muweilih areas, Qift-Quseir Road, Eastern Desert, Egypt. Ph.D. Thesis, Faculty of Science, Al Azher University, Cairo-Egypt, pp. 308.

Khudeir, A.A., 1995. Chromian spinel-silicate chemistry in peridotite and orthopyroxenite relicts from ophiolitic serpentinites, Eastern Desert, Egypt. Bulletin of Faculty of Science, Assiut University 24, 221–261.

Khudeir, A.A., Asran, H.A., 1992. Back-arc Wizr ophiolites at Wadi Um Gheig District, Eastern Desert, Egypt. Bulletin of Faculty of Science, Assiut University 21 (2-F), 1–22.

Khudeir, A.A., El Haddad, M.A., Leake, B.E., 1992. Compositional variation in chromite from the Eastern Desert, Egypt. Mineralogical Magazine 56, 567–574.

Kröner, A., Reischmann, T., Wust, H.J., Rashwan, A.A., 1988. Is there any pre-Pan-African (>950 Ma) basement in the Eastern Desert of Egypt? In: El Gaby, S., Greiling, R.O. (Eds.), The Pan-African Belt of northeast Africa and adjacent areas. Braunschweig Viewig, pp. 95–119.

Leblanc, M., Dupuy, C., Cassard, D., Noutte, J., Nicolas, A., 1980. Essai sur la genese des corps podiformes de chromite dans les peridotites ophiolitiques: etude des chromites de Nouvelle. In: A. Panayiotou (ed), Ophiolites Proceedings International Symposium Cyprus. Geological Survey Department, Cyprus Publication, pp. 691–701.

Murton, B.J., 1989. Tectonic controls on boninite genesis. In: Saunders, A.D. and Norry, M.J. (eds) Magmatism in the ocean basins. Geological Society of London, Special Publication 42, pp. 347–377.

Newton, R.C., Stern, R.J., 1990. A Late Precambrian CO_2 "Event". Geological Society of America, Dallas, p. 190.

Ohara, Y., 2006. Mantle Process beneath Philippine Sea back-arc spreading ridges: A synthesis of peridotite petrology and tectonics. The Island Arc 15, 119–129.

Ohara, Y., Ishii, T., 1998. Peridotites from southern Mariana forearc: Heterogeneous fluids supply in mantle wedge. The Island Arc 7, 541–558.

Ohara, Y., Stern, R.J., Ishii, T., Yurimoto, H., Yamazaki, T., 2002. Peridotites from the Mariana Trough: first look at the mantle beneath an active back-arc basin. Contribution to Mineralogy and Petrology 143, 1–18.

Pal, T., Mitra, S., 2004. P-T-fO$_2$ controls on a partly inverse chromite-bearing ultramafic intrusive: an evaluation from the Sukinda Massif, India. Journal of Asian Earth Sciences 22, 483–493.

Parkinson, I.J., Pearce, J.A., 1998. Peridotites from the Izu-Bonin-Mariana forearc (ODP Log 125): evidence for mantle melting and melt-mantle interaction in a supra-subduction zone setting. Journal of Petrology 39, 1577–1618.

Pearce, J.A., Lippard, S.J., Roberts, S., 1984. Characteristics and tectonic significance of supra-subduction zone ophiolites. In: Kokelaar, B.P., Howells, M.F. (Eds.), Marginal Basin Geology. Geological Society. Special Publication 16, 1984, pp. 77–94.

Pearce, J.A., Barker, P.F., Edwards, S.J., Parkinson, I.J., Leat, P.T., 2000. Geochemistry and tectonic significance of peridotites from the South Sandwich arc-basin system, South Atlantic. Contribution to Mineralogy and Petrology 139, pp. 36–53.

Ries, A.C., Shackleton, R., Graham, R.H., Fitches, W.R., 1983. Pan-African structures, ophiolites and mélanges in the Eastern Desert of Egypt: a traverse at 26° N. Journal of Geological Society of London 140, 75–95.

Roberts, S., 1992. Influence of partial melting regime on the formation of ophiolitic chromite. In: Parson, L.M., Murton, B.J., Browning, P. (Eds.), ophiolites and their Modern Oceanic Analogues. Geological Society, Special Publication, 6, pp. 203–217.

Sack, R.O., Ghiorso, M.S., 1991. Chromian spinels as petrogenetic indicators: thermodynamics and petrologic applications. American Mineralogist 76, 827–847.

Salem, I.A., Ghoneim, M.F., Zahran, A.A., Hamdy, M.M., 1997. Petrology and genesis of the ultramafic-hosted vein magnesite deposits at G. El-Rubshi, central Eastern Desert, Egypt. In: The 3rd International Conference on Geochemistry, Alexandria University, pp. 241–267.

Shackleton, R.M., 1994. Review of late Proterozoic sutures, ophiolitic mélanges and tectonics of eastern Egypt and north Sudan. Geological Rundschau 83, 537–546.

Shackleton, R.M., Ries, A.C., Graham, R.H., Fitches, W.R., 1980. Late Precambrian ophiolitic mélange in the Eastern Desert of Egypt. Nature 285, 472–474.

Sobolev, N.V., Logvinova, A.M., 2005. Significance of accessory chrome spinels in identifying serpentinite paragenesis. International Geological Review 47, 58–64.

Stacey, J.S., Stoeser, D.B., 1983. Distribution of oceanic and continental leads in the Arabian–Nubian Shield. Contribution to Mineralogy and Petrology 84, 91–105.

Stern, R.J., Bloomer, S.H., 1992. Subduction zone infancy: examples from the Eocene Izu-Bonin-Mariana and Jurassic California arcs. Geological Society of America Bulletin 104, 1621–1636.

Stern, R.J., Gwinn, C.J., 1990. Origin of late Precambrian intrusive carbonates, Eastern Desert of Egypt and Sudan: C, O and Sr isotopic Evidence. Precambrian Research 46, 259–272.

Stern, R.J., Hedge, C.E., 1985. Geochronologic and isotopic constraints on Late Precambrian crustal evolution in the Eastern Desert of Egypt. American Journal of Sciences 285, 97–127.

Stern, R.J., Johnson, P.R., Kröner, A., Yibas, B., 2004. Neoproterozoic ophiolites of the Arabian–Nubian Shield. In: Kusky, T.M. (ed.), Precambrian Ophiolites and Related Rocks. Developments in Precambrian Geology 13, pp. 95–128.

Sultan, M., Bickford, M.E., El Kaliouby, B., Arvidson, R.E., 1992. Common Pb systematics of Precambrian granitic rocks of the Nubian Shield (Egypt) and tectonic implications. Geological Society of American Bulletin 104, 456–470.

Surour, A.A., Arafa, E.H., 1997. Ophicarbonates: calcified serpentinites from Gebel Moghara Wadi Ghadir area, Eastern Desert, Egypt. Journal of African Earth Sciences 24, 315–324.

Takla, M.A., El Sharkawy, M.A., Basta, F.F., 1982. Petrology of the basement rocks of Gabal Mohagara-Ghadir area, Eastern Desert, Egypt. Annals of the Geological Survey of Egypt 12, 121–140.

Wust, H.J., Todt, W., Kröner, A., 1987. Conventional and single grain zircon ages for metasediments and granite clasts from the Eastern Desert of Egypt: evidence for active continental margin evolution in Pan-African times. Terra Cognita 7, 165 (Abstract).

Zimmer, M., 1989. Der Gebel-Gerf Komplex (Arabisch–Nubischer-Shield): Petrographische und geochemische Undersuchugen eins Späproteroischen Ophiolithes. Thesis, University of Mainz, Germany, pp. 192.

Zimmer, M., Kröner, A., Jochum, K.P., Reischmann, T., Todt, W., 1995. The Gabal Gerf complex: a Precambrian N-MORB ophiolite in the Nubian Shield, NE Africa. Chemical Geology 123, 29–51.